Determination of the Se Atom Distribution in the Layered Compound $Nb_3(Se_{1-x}I_x)I_7$ by Scanning Tunneling Microscopy

Peter J. Schmidt,[a] Gerhard Thiele,*[a] and Myung-Hwan Whangbo*[b]

Keywords: Atom distribution / Mixed crystals / Scanning tunneling microscopy / Layered compounds

The layered compound $Nb_3(Se_{1-x}I_x)I_7$ is obtained when the I atoms at the face-capping sites of the layered compound Nb_3I_8 are replaced by Se atoms. The amount and distribution of the Se atoms in $Nb_3(Se_{1-x}I_x)I_7$ were examined by scanning tunneling microscopy. The analysis shows that the distribution of the Se atoms is completely random.

It is a challenging problem to study how chemical substitution or doping affect the structural and electronic properties of a material at the atomic level. A local-probe technique such as scanning tunneling microscopy (STM)[1][2] provides information about localized defects of a modified material, as demonstrated in a number of STM studies on layered compounds[3−6] and alloys.[7][8] Recently, a number of ternary compounds Nb_3YX_7 (X = halogen, Y = chalcogen) have been prepared.[9] As shown for $Nb_3S_{1-x}I_{7+x}$,[10] a wide range of mixed crystals between Nb_3X_8 and Nb_3YX_7 can be obtained. These compounds are related to the layered halides Nb_3X_8 (X = Cl, Br, I),[11] whose building block is an Nb_3X_{13} cluster (Figure 1a). Nb_3X_8 layers are obtained from these clusters upon sharing their outer octahedral edges (Figure 1b) in such a way that the two surfaces of an Nb_3X_8 layer are different: One surface (surface A) has the triangular face of each Nb_3 trimer capped by the X(4) atom, while the other surface (surface B) has the edges of each Nb_3 trimer capped by the X(1) atoms. The layers of Nb_3X_8 are stacked such that the interface between adjacent layers consists of either surface A or surface B (Figure 1c). Our single-crystal X-ray diffraction analysis of different $Nb_3Se_{1-x}I_{7+x}$ samples shows that only the face-capping site, i.e., I(4), is replaced by Se. When $0 < x < 1$, the face-capping sites of $Nb_3Se_{1-x}I_{7+x}$ are occupied by either I or Se so that each $Nb_3Se_{1-x}I_{7+x}$ layer consists of Nb_3I_{13} and Nb_3SeI_{12} clusters. In this paper, we demonstrate that the amount and distribution of the Se atoms in $Nb_3Se_{1-x}I_{7+x}$ can be determined by STM.

Typical STM images of $Nb_3Se_{1-x}I_{7+x}$ are divided into two groups, A and B, because the surface of the $Nb_3Se_{1-x}I_{7+x}$ sample mounted on the support can be either surface A or surface B. The STM images of group A show patterns of three bright and one less bright spots per unit cell (Figure 2a). This pattern can be readily seen by filtering the observed image by the two-dimensional fast Fourier transform procedure, as illustrated on the upper left part of Figure 2a. The STM images of group A exhibit image defects as dark spots that have the size of approximately one cluster unit. The STM images of group B show one bright spot for each unit cell, with varying degrees of brightness (Figure 2b). The STM images of group A and B recorded for $Nb_3Se_{1-x}I_{7+x}$ refer to the surfaces A and B, respectively. When the image defects are neglected, their unit cell patterns are similar in pattern to the partial density plots $\rho(r_0, E_f)$ calculated for surfaces A and B of Nb_3I_8, respectively.[12]

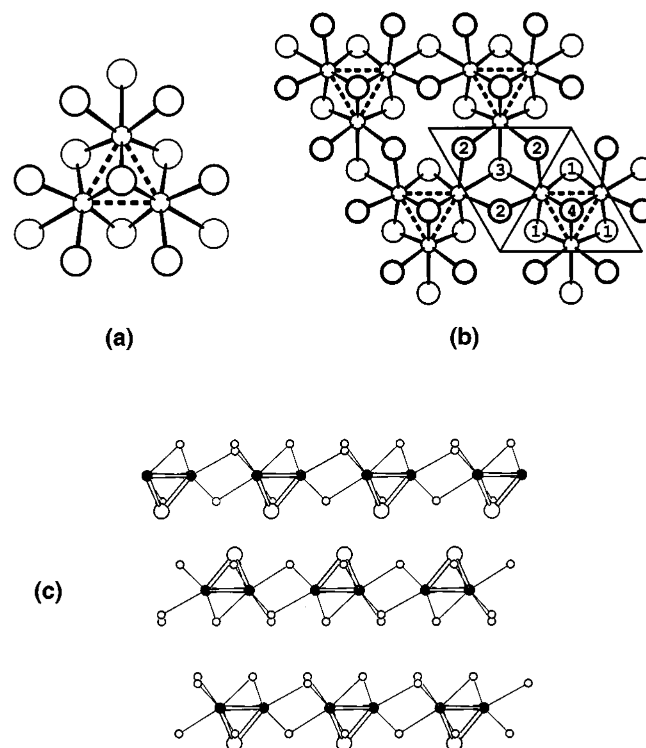

Figure 1. (a) Perspective view of an $[Nb_3X_{13}]^{5-}$ cluster, where the small and large circles represent Nb and X atoms, respectively; (b) top, (001) projection of a single Nb_3X_8 layer; the X(4) and X(1) atoms occupy the face- and edge-capping sites of each Nb_3 cluster, respectively; the X(2) atoms bridge two clusters, and the X(3) atoms connect three Nb_3 clusters; (c) schematic projection view of how the Nb_3X_8 layers stack in Nb_3I_8; the shaded circles represent the Nb atoms, the large open circles the X(4) atoms, and the small open circles all other X atoms

Figures 3a and 3c show representative STM images recorded for the surface B of $Nb_3Se_{0.24}I_{7.76}$. The image of Figure 3a was obtained with $I_{set\text{-}point}$ = 3.82 nA and V_{bias} =

[a] Institut für Anorganische und Analytische Chemie and Materialforschungszentrum (FMF), Albert-Ludwigs-Universität, Stefan-Meier-Strasse 21a, D-79104 Freiburg, Germany
[b] Department of Chemistry, North Carolina State University, Raleigh, North Carolina 27695-8204, USA

 © WILEY-VCH Verlag GmbH, D-69451 Weinheim, 1999 1434−1948/99/0505−0785 $ 17.50+.50/0

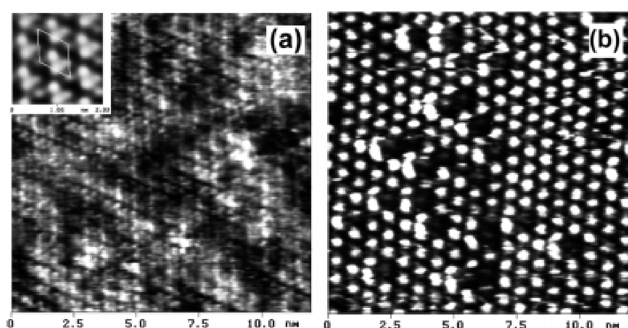

Figure 2. (a) STM current image of $Nb_3Se_{0.36}I_{7.64}$ (V_{bias} = −164.8 mV, $I_{set\text{-}point}$ = 19.89 nA); (b) STM current image of $Nb_3Se_{0.09}I_{7.91}$ (V_{bias} = −300 mV, $I_{set\text{-}point}$ = 3.48 nA)

−517.9 mV, and that of Figure 3c with $I_{set\text{-}point}$ = 15.98 nA and V_{bias} = −481.3 mV. The tip-sample distance in contact-mode STM decreases with decreasing the resistance gap, $R_{gap} = |V_{bias}|/I_{set\text{-}point}$.[2d] Thus, the strength of the tip-sample repulsive interaction, and hence the extent of the sample indentation induced by the tip force, increases with decreasing R_{gap}.[2d] The values of R_{gap} used to obtain the STM images of Figures 3a and 3c are 135.6 and 30.12 MΩ, respectively, so that the tip-sample repulsive interaction leading to the STM image of Figure 3c was much stronger than that leading to the STM image of Figure 3a. To see how often the spot of any given contrast occurs in the STM image of Figure 3a, the contrast of each spot in this image was analyzed. The histogram of Figure 3b shows how many times (in relative number) the spot of a certain contrast occurs as a function of the contrast. The corresponding analysis carried out for the STM image of Figure 3c is summarized in Figure 3d. The bright and less bright spots are more clearly separated in Figure 3d than in Figure 3b. As will be shown below, the concentration ratio [Se]/[I(4)] in $Nb_3Se_{1-x}I_{7+x}$, which is given by $(1 - x)/x$, is equal to the number ratio of the dark spots to the bright spots in the STM images of group B. Thus, the difference between the Nb_3I_{13} and Nb_3SeI_{12} clusters in $Nb_3Se_{1-x}I_{7+x}$ is more clearly distinguished when the tip-sample force interaction is stronger. The reason for this observation will be discussed in our forthcoming paper.[13]

The above discussion shows that the content and distribution of Se in $Nb_3Se_{1-x}I_{7+x}$ can be detected by STM. To examine the nature of the Se atom distribution in $Nb_3Se_{1-x}I_{7+x}$, we analyzed the STM images recorded for the surface B of $Nb_3Se_{1-x}I_{7+x}$. It is easy to assign whether a given spot of the STM image is associated with the Nb_3I_{13} or the Nb_3SeI_{12} cluster; consequently, a given STM image can be converted into a digitized image consisting solely of bright and dark circles representing the Nb_3I_{13} and Nb_3SeI_{12} clusters, respectively. For instance, Figure 4 shows four digitized images obtained from the STM images determined on four different surface regions of $Nb_3Se_{0.24}I_{7.76}$. The amount of Se determined from the digitized images is in good agreement with that determined by wavelength-dispersive X-ray (WDX) analysis. In the digitized images, bright and dark circles form a hexagonal lattice in which each circle is surrounded with six nearest neighbor circles.

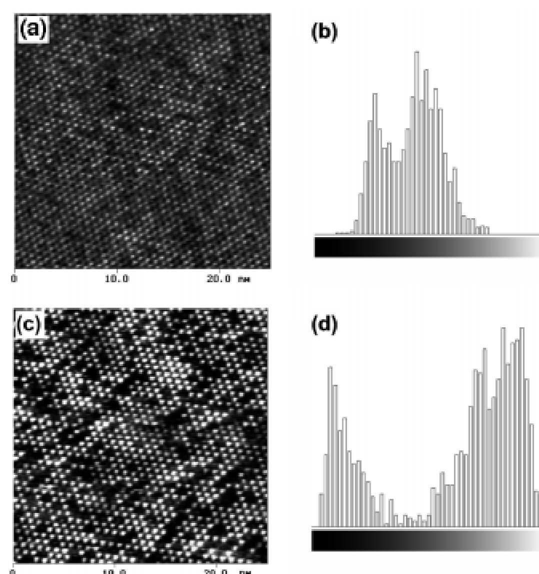

Figure 3. (a) STM current image recorded for surface B of $Nb_3Se_{0.24}I_{7.76}$ ($I_{set\text{-}point}$ = 3.82 nA, V_{bias} = −517.9 mV); (b) histogram of how often the spot of any given contrast occurs in the STM image of (a); (c) STM current image recorded for surface B of $Nb_3Se_{0.24}I_{7.76}$ ($I_{set\text{-}point}$ = 15.98 nA, V_{bias} = −481.3 mV); (d) histogram of how often the spot of any given contrast occurs in the STM image of (c); the images of (a) and (c) were obtained from the same sample surface, but the positions are not the same due to the thermal drift during the measurements; the contrast variations in (a) and (c) cover the same range and are proportional to ln I

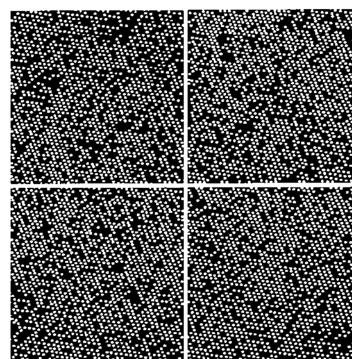

Figure 4. Digitized images derived from analyzing surface B STM images of $Nb_3Se_{0.24}I_{7.76}$ (30 nm × 30 nm); bright and dark spots refer to the Nb_3I_{13} and Nb_3SeI_{12} clusters, respectively

To determine if the distribution of the Se atoms is random, we examined each dark circle of the digitized image and counted how many of its nearest neighbor circles are dark circles. If the distribution of the Se atoms in $Nb_3Se_{1-x}I_{7+x}$ is truly random, then the probability $p(m)$ of finding m = 0, 1, 2, 3, 4, 5, or 6 dark circles as nearest neighbors of a given dark circle can be described by a binomial distribution (Equation 1)

$$p(m) = [6!/m!(6 - m)!](1 - x)^m(x)^{6-m} \quad (1)$$

The $p(m)$ values predicted by Equation 1 are compared with the experimental values determined by analyzing the

digitized images of $Nb_3Se_{0.24}I_{7.76}$ in Figure 5, which shows an excellent agreement between the theoretical and experimental $p(m)$ values. The same result is obtained with samples of different Se content. Thus, the distribution of the Se atoms in $Nb_3Se_{1-x}I_{7+x}$ is random.

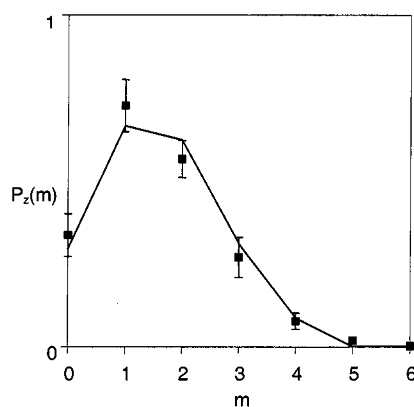

Figure 5. Comparison of the theoretical and experimental $p(m)$ values determined for the distribution of the Se atoms in $Nb_3Se_{0.24}I_{7.76}$

In summary, we determined the content and distribution of Se in $Nb_3Se_{1-x}I_{7+x}$ by carrying out STM experiments. Our work shows that the Nb_3I_{13} and Nb_3SeI_{12} clusters are distinguished by STM, and that the distribution of the Se atoms in $Nb_3Se_{1-x}I_{7+x}$ is random.

Experimental Section

Single crystals of $Nb_3Se_{1-x}I_{7+x}$ were obtained by heating mixtures of the elements in evacuated sealed silica tubes as described in ref.[11b] To avoid the twinning of crystals, the tubes were rapidly quenched at the end of reaction. Higher niobium iodides and niobium selenide iodides were separated from the desired product by sublimation before opening the tubes. The purity and homogeneity of the products were checked by powder X-ray diffraction. The structure and chemical composition of the products were determined by single-crystal X-ray diffraction analysis and by WDX analysis using β-Nb_3I_8 and LT-$NbSe_2I_2$[14] as standards. Samples of $Nb_3Se_{1-x}I_{7+x}$ were examined by STM, as described for Nb_3I_8 elsewhere.[12] Contact-mode STM measurements were carried out on freshly cleaved surfaces of the mounted crystal samples at ambient conditions using a commercial scanning probe microscope Nanoscope II (Digital Instruments, Inc.), mechanically sharpened Pt/Ir 70:30 tips for STM, and commercial cantilevers with Si_3N_4 probes for AFM.

Acknowledgments

The work at North Carolina State University was supported by the Office of Basic Energy Sciences, Division of Materials Sciences, U. S. Department of Energy, under Grant DE-FG05−86ER45259. The work at Freiburg University was financially supported by the Deutsche Forschungsgemeinschaft (DFG) and the Fonds der Chemischen Industrie.

[1] G. Binnig, H. Rohrer, C. Gerber, E. Weibel, *Phys. Rev. Lett.* **1982**, *49*, 57.
[2] [2a] R. Wiesendanger, H.-J. Güntherodt, *Scanning Tunneling Microscopy I, II and III*, Springer, Heidelberg, **1992** and **1993**. − [2b] C. J. Chen, *Introduction to Scanning Tunneling Microscopy*, Princeton University Press, Princeton, **1993**. − [2c] D. A. Bonnell, *Scanning Tunneling Microscopy and Spectroscopy*, VCH, New York, **1993**. − [2d] S. N. Magonov, M.-H. Whangbo, *Surface Analysis with STM and AFM*, VCH, Weinheim, **1996**.
[3] B. A. Parkinson, *J. Am. Chem. Soc.* **1990**, *112*, 1030.
[4] H. Dai, C. M. Lieber, *J. Phys. Chem.* **1993**, *97*, 2362.
[5] [5a] P. J. Schmidt, *Diploma Thesis*, Freiburg University, **1996**. − [5b] H. Hillebrecht, P. J. Schmidt, H. W. Rotter, G. Thiele, P. Zönnchen, H. Bengel, H.-J. Cantow, S. N. Magonov, M.-H. Whangbo, *J. Alloys Comp.* **1997**, *246*, 70.
[6] X. Lu, K. W. Hipps, X. D. Wang, U. Mazur, *J. Am. Chem. Soc.* **1996**, *118*, 7197.
[7] M. Schmid, H. Stadler, P. Varga, *Phys. Rev. Lett.* **1993**, *70*, 1441
[8] P. T. Wouda, B. E. Nieuwenhuys, M. Schmid, P. Varga, *Surf. Sci.* **1996**, *359*, 17
[9] [9a] S. Furuseth, W. Hönle, G. J. Miller, H. G. von Schnering, *9th International Conference on Solid Compounds of Transition Elements, Abstracts*, Royal Society of Chemistry, London, **1988**. − [9b] G. V. Khvorykh, A. V. Shevelkov, V. A. Dolgikh, B. A. Popovkin, *J. Solid State Chem.* **1995**, *120*, 311. − [9c] G. J. Miller, *J. Alloys Comp.* **1995**, *217*, 5. − [9d] G. J. Miller, *J. Alloys Comp.* **1995**, *229*, 93.
[10] [10a] C.-S. Lee, *M. Sc. Thesis*, Iowa State University, **1997**. − [10b] G. J. Miller, J. Lin, M. D. Smith, C. S. Lee, to be published.
[11] [11a] H. G. von Schnering, H. Wöhrle, H. Schäfer, *Naturwissenschaften* **1961**, *48*, 159. − [11b] A. Simon, H. G. von Schnering, *J. Less-Common Met.* **1966**, *11*, 31. − [11c] F. Hulliger, *Structural Chemistry of Layer-Type Phases* (Ed.: F. Lévy), Reidel, Dordrecht, The Netherlands, **1976**.
[12] S. N. Magonov, P. Zönnchen, H. W. Rotter, G. Thiele, H.-J. Cantow, J. Ren, M.-H. Whangbo, *J. Am. Chem. Soc.* **1993**, *115*, 2495.
[13] P. J. Schmidt, G. Thiele, H. -J. Cantow, J. Ren, M.-H. Whangbo, in preparation.
[14] J. Rijnsdorp, G. J. De Lange, G. A. Wiegers, *J. Solid State Chem.* **1979**, *30*, 365.

Received December 15, 1998
[I98432]